

Exposing the spin glass ground state of the non-superconducting $\text{La}_{2-x}\text{Sr}_x\text{Cu}_{1-y}\text{Zn}_y\text{O}_4$ high- T_c oxide

C. Panagopoulos¹, A.P. Petrovic¹, A.D. Hillier²,
 J.L.Tallon³, C.A. Scott⁴, and B.D. Rainford⁴

¹ *Cavendish Laboratory and Interdisciplinary Research Centre in Superconductivity,
 University of Cambridge, Cambridge CB3 0HE, United Kingdom*

² *Rutherford Appleton Laboratory, Chilton Didcot,
 Oxfordshire OX11 0QX, United Kingdom*

³ *MacDiarmid Institute for Advanced Materials and Nanotechnology,
 Industrial Research Ltd, P.O. Box 31310, Lower Hutt, New Zealand and*

⁴ *Department of Physics and Astronomy, University of Southampton,
 Southampton SO17 1BJ, United Kingdom*

(Dated: November 9, 2018)

Abstract

We have studied the spin glass behaviour of non-superconducting $\text{La}_{2-x}\text{Sr}_x\text{Cu}_{0.95}\text{Zn}_{0.05}\text{O}_4$ ($x = 0.10 - 0.22$). As in the superconducting analogues of these samples the spin glass transition temperature T_g decreases with increasing x , and vanishes at $x = 0.19$. A local enhancement in T_g at $x = 0.12$ is also observed and attributed to stripe ordering. The disappearance of T_g for $x \geq 0.19$ is discussed in terms of a quantum phase transition.

The prototype oxide La_2CuO_4 is an example of a diluted quantum antiferromagnet in which the Neel temperature decreases with doping and added holes are believed to segregate, at first, into stripes^{1,2,3,4}. La_2CuO_4 undergoes an insulator-superfluid transition by hole doping, and this is generally explored by replacing La^{3+} with Sr^{2+} to form $\text{La}_{2-x}\text{Sr}_x\text{CuO}_4$. Early works indicated that for $x > 0.01$ $\text{La}_{2-x}\text{Sr}_x\text{CuO}_4$ changes from a long-range antiferromagnetic insulator to a spin glass, characterised by a cusp in magnetisation at the glass transition temperature T_g and an associated field hysteresis below^{5,6,7,8}. The critical exponents and memory effect were found to be in good agreement with conventional spin glass systems, although a crystallographic directional dependence, possibly related to the presence of stripes, was observed. Nevertheless, the onset of spin glass behaviour in all three principle crystallographic directions was shown to be associated with an order parameter and broken symmetry due to frozen spins^{9,10}.

Similar magnetisation studies cannot be performed for $x > 0.05$ due to masking of the thermodynamic spin glass characteristics by the onset of superconducting diamagnetism. However, other reliable methods such as neutron scattering, nuclear magnetic resonance and muon spin relaxation (μSR) have been successfully employed to investigate spin glass behaviour across the (T, x) phase diagram of HTS^{6,8,11,12,13,14,15,16,17,18,19,20,21,22,23,24,25,26}. Although T_g obtained from spectroscopic techniques may vary depending on their frequency window there is good agreement with thermodynamic measurements where available. Over the past several years various spectroscopic studies have shown T_g to extend into the superconducting dome of the HTS phase diagram indicating coexistence of superconducting and spin glass order. Furthermore, a comprehensive μSR study in several HTS showed that T_g ceases to exist at a critical doping $x_c \simeq 0.20$ suggesting the presence of a quantum glass transition^{24,25,26}.

However, it remains to be confirmed that x_c is in fact robust with respect to the energy window of μSR . That is, if the absence of dynamical relaxation for $x > x_c$ is independent of the energy scale of the spin fluctuations, hence the presence of an unambiguous quantum transition. To address this question we have exposed the normal state magnetic ground state of $\text{La}_{2-x}\text{Sr}_x\text{CuO}_4$ across the superconducting dome. Instead of using an applied field, which is beyond experimental capabilities, we use non-magnetic Zn, to suppress superconductivity. Substituting zinc for copper also slows down the spin fluctuations, suppresses long range order, and on the basis of systematic μSR studies it enhances the muon depolarisation

rate at low temperatures and increases $T_g^{25,27}$. These effects allow us to eliminate possible masking of a short-range magnetic order due to the μ SR frequency limit. A disadvantage in using zinc is that the exposed ground state is distorted and therefore not pristine. However, this does not affect the aim of the present work since we are mainly interested in the evolution of short-range magnetic order.

The materials studied were $\text{La}_{2-x}\text{Sr}_x\text{Cu}_{0.95}\text{Zn}_{0.05}\text{O}_4$ ($x=0.10-0.22$). Samples were synthesised using solid-state reaction and where necessary followed by quenching and subsequent oxygenation. Spectroscopic, chemical and elemental analyses showed them to be phase pure and stoichiometric. Magnetisation measurements indicated $T_c=0$ in all samples. Zero-field (ZF) and longitudinal-field (LF) μ SR studies were performed at the pulsed muon source, ISIS Facility, Rutherford Appleton Laboratory. In a μ SR experiment, 100% spin-polarised positive muons implanted into a specimen precess in their local magnetic environment. Random spin fluctuations will depolarise the muons provided they do not fluctuate much faster than the muon precession. The muon decays with a life-time $2.2\mu\text{s}$, emitting a positron preferentially in the direction of the muon spin at the time of decay. By accumulating time histograms of such positrons one may deduce the muon depolarisation rate as a function of time after implantation. The muon is expected to reside at the most electronegative site of the lattice. As discussed previously in $\text{La}_{2-x}\text{Sr}_x\text{Cu}_{1-y}\text{Zn}_y\text{O}_4$ it is the apical O^{2-} nearest to the planes so the results reported here are dominated by the magnetic correlations within the CuO_2 planes^{25,28}.

Figure 1 (left-hand-side panels) shows the time dependence of the ZF muon asymmetry for $\text{La}_{2-x}\text{Sr}_x\text{Cu}_{0.95}\text{Zn}_{0.05}\text{O}_4$ with $x=0.10 - 0.18$. All samples exhibit glassy behaviour with $x = 0.18$ (at $T = 0.03\text{K}$) being just at the threshold of glassiness. A characteristic signature of a spin-glass within a μ SR spectrum is a rapid initial relaxation followed by a much slower and more gradual long-term relaxation²⁹. This can be explained by considering the muon lifetime within the glass: upon insertion, the spin-polarised muons are greeted by a distribution of randomly aligned magnetic fields. Since these fields are quasi-static the detected asymmetry relaxes very quickly. The ensuing longer-term relaxation is due to a small number of low-frequency fluctuations, which may still be present in the CuO_2 planes of the samples. Let us note that in a typical spin glass system a single pronounced dip is expected after the sharp drop in asymmetry²⁹. However, this behaviour is not universal among systems exhibiting short range ordered magnetism, including HTS, and should not be viewed

as the essential condition for characterising spin glass behaviour^{13,14,15,16,17,24,25,26,29,30}. Furthermore, as discussed above, other studies in HTS such as neutron scattering and nuclear magnetic resonance, also show clear evidence for spin glass behaviour. Most importantly however, it is in the temperature region where the ZF μ SR spectrum shows the rapid initial relaxation that thermodynamic measurements exhibit a well-defined field-dependent magnetic transition and associated thermal hysteresis at T_g , indicating glassy short-range magnetic ordering with an associated order parameter^{5,6,7,8}. The right-hand-side panels of Fig. 1 depict typical spectra obtained with an external longitudinal field applied parallel to the initial muon spin polarisation. The field dependence of the spectra indicates that the spins depolarising the muons are static and as the applied field increases the depolarisation decreases and the asymmetry eventually recovers its initial value.

The $x=0.18$ sample displays a much slower relaxation compared with $x < 0.18$ but still clearly indicates the presence of a glass at the lowest temperature ($T=0.03\text{K}$). It shows three characteristic indications that it has already entered the glassy phase. Firstly, the spectrum relaxes much quicker than the heavily over-doped samples; secondly, it follows the field dependence of samples $x=0.10 - 0.16$ and thirdly, the rate of change of the gradient in the asymmetry spectrum (*i.e.* the second derivative) is positive rather than negative. The spectra for $x \geq 0.19$ were Gaussian at all temperatures (see e.g. Fig. 2(a)).

The inset for the ZF-plot for $x = 0.10$ in Fig. 1 shows ZF-data for $x=0.10$ and 0.12 at short-times. We find that at very small time scales $x = 0.10$ and $x = 0.12$ (multiplied by 1.3 for clarity) exhibit a faint oscillation which quickly fades as time increases. These oscillations are enhanced at lower temperatures and doping and are successfully fitted by including a precessing component in the Kubo-Toyabe function^{17,31,32,33}. Oscillations are only observed for $x < 0.13$ and $y = 0 - 0.05$ and can only be due to the precession of the muon spins around a stronger non-random internal field caused by the presence of an ordered magnetic state. For example, an antiferromagnetic ground state may be present here. This has also been inferred from neutron scattering experiments for $x=0.11$ ³⁴. We speculate that these oscillations may be related to the presence of stripes^{17,31,32,33}. At this doping range most HTS show a small drop or a plateau in T_c and in the superfluid density^{24,25,35}. The exact reason for this drop is unclear, but it is thought that there is an enhanced tendency towards magnetic ordering at this point due to some peculiarity in the structural orientation of the CuO_6 octahedra. This has the effect of creating strongly correlated antiferromagnetic stripe domains. It is these

stripes which may provide the spin correlations causing the muon precession. This stripe arrangement is reminiscent of the antiferromagnetic phase present for $x < 0.02$ and raises the question as to whether there is a hidden weak antiferromagnetic ground state present in other regions of the phase diagram of $\text{La}_{2-x}\text{Sr}_x\text{CuO}_4$. Further investigations on this matter are to be carried out.

As the temperature is increased, samples displaying glassy behaviour exhibit a gradual change in the spectra. A typical example, $x = 0.10$, is shown in Fig. 2(c). In glassy samples ($x < 0.19$), at high temperature the depolarisation is Gaussian and temperature independent, just like $x \geq 0.19$, consistent with dipolar interactions between the muons and their near-neighbour nuclear moments. This was verified by applying a small longitudinal magnetic field (30G) to the $x=0.14$ sample at 50K in order to ascertain the origin of the muon response (Fig. 2(d)). The field due to the nuclear moments is extremely weak (much weaker than the internal field present for a spin-glass). Therefore, nuclear decoupling leading to a collapse in the response function should result following application of even a very low field as shown in Fig. 2(d). The Gaussian behaviour at high temperature was verified also for the samples with lower hole-dopings. Furthermore, a 30G field was also applied to the $x=0.19$ sample at $T=0.03\text{K}$ and 0.75K to check for nuclear decoupling (Fig. 2(b)). The muon response was again observed to collapse, for the same field at both temperatures, showing that there is no evidence for low-energy electron spin fluctuations or onset of glassy behaviour for $x \geq 0.19$.

As in earlier works^{24,25,26}, two characteristic temperatures for use in the analysis of the slowing of the spin fluctuations have been determined. These are the temperature T_f where the spin correlations first enter the μSR time window, *i.e.* where the muon asymmetry first deviates from Gaussian behaviour and the temperature T_g at which these correlations freeze into a glassy state thus causing an initial rapid decay in the asymmetry. The evolution of the muon spin with time (*i.e.* its relaxation) may be fitted to the form $G_z(t) = A_1 \exp(-\lambda_1 t) + A_2 \exp(-(\lambda_2 t)^\beta) + A_3$ where the first term is the fast relaxation in the glassy state (*i.e.* $A_1=0$ for $T > T_g$), the second stretched-exponential term describes the slower relaxation of the dynamical spins and A_3 accounts for a small time-independent background arising from muons stopping in the silver backing plate of the sample holder. As in some other spin glass systems, β is constant (with the value $\beta=2$) in the high-temperature Gaussian limit (Fig. 3)^{29,30}. The temperature where β starts decreasing (Fig. 3) and the spin lattice relaxation

rate λ increasing (*e.g.* Fig. 3 (inset to $x=0.10$)) is regarded as the onset temperature, T_f , at which spin fluctuations slow down sufficiently to enter the frequency scale of the muon probe (10^{-10}s).

Now, to address the question of a possible quantum phase transition at x_c , we concentrate on the freezing temperature, T_g , for which thermodynamic measurements indicate an associated spin glass order parameter. In ZF- μSR T_g is identified as the temperature where β falls to 0.5 ± 0.06 ³⁰. This root exponential form for the relaxation function is a common feature of spin glasses. It should be noted that different fitting procedures for estimating T_g consistently yield similar values^{25,36,37}. It is also at $\beta=0.5$ where the spin lattice relaxation rate, as obtained from the same fits, reaches a maximum, as shown in the inset to Fig. 3 for $x=0.10$. This confirms μSR as a credible technique to accurately identify and characterise spin-glass behaviour. Figure 3 shows the variation of β with temperature for some of the samples studied. At first glance we see the onset (where β starts falling) and freezing of spin fluctuations vary in the same manner as found for pure, 1 and 2 % Zn doped $\text{La}_{2-x}\text{Sr}_x\text{CuO}_4$, *i.e.*, decreasing with increasing doping. Furthermore, for $x \geq 0.19$, there are no changes in the depolarisation function and β is almost temperature independent, consistent with Gaussian depolarisation. It is clear from the data that changes in the magnetic ground state occur at $x = 0.19$. The main contribution of the present study is that superconductivity has been fully suppressed and therefore any masked or hidden magnetism is now exposed. This was important to demonstrate experimentally since earlier works left question marks as to whether changes in the measured magnetic ground state were reflecting actual changes in ground state of the material, or were an artefact of the presence of superconductivity.

Values of T_g summarised in Fig. 4 indicate a gradual decrease of the onset of the spin glass phase with doping. The exception is the $x = 0.12$ sample for which T_g is higher than for $x = 0.10$. We note the positive curvature of $T_g(x)$, exactly as seen previously for pure, 1 and 2 % Zn doped $\text{La}_{2-x}\text{Sr}_x\text{CuO}_4$ and pure $\text{Bi}_{2.1}\text{Sr}_{1.9}\text{Ca}_{1-x}\text{Y}_x\text{Cu}_2\text{O}_{8+y}$, and expected in quasi-2D systems like the HTS^{24,25,26}. The increase in T_g in the 1/8 region has been previously discussed in terms of stripe domains^{24,25,26,31,33}. The effect of the ordered phase is also evident for $x = 0.14$, which from the trend of $T_g(x)$ indicates the latter is higher than expected for this doping. In fact the presence of a static stripe component for $x = 0.14$ can be seen in neutron scattering experiments^{35,38}. Here the order parameter is small and is unlikely to be homogeneous which is consistent with the absence of a well-defined precession frequency in

our μ SR measurements. The spin glass regime vanishes at $x = 0.19$ and for $x \geq 0.19$ we did not observe even an onset (T_f) of spin fluctuations slowing down sufficiently to enter the frequency scale of the muon probe (Fig. 4). The field dependent studies (see e.g. Fig. 1) enabled us estimate the internal local field, B_{local} , sensed by the implanted muons³⁹. Fig. 4 also includes the doping dependence near x_c of B_{local} , measured at $T = 0.03$ K. This exhibits a behavior similar to T_g and T_f and disappears at precisely $x = 0.19$.

The observation $T_{g,f}(x)=0$ and $B_{local}=0$, at $x \geq 0.19$ *for all Zn concentrations* indicates that spin glass and low frequency fluctuations disappear at x_c and earlier results to this effect were not masked by either the frequency window of the technique or the presence of superconductivity. Similar conclusions have been reached by recent Cu-nuclear quadrupole resonance studies⁴⁰. Bearing in mind the fact that T_f and $T_g \rightarrow 0$ at $x = 0.19$ so that the rate of slowing down actually diverges at this point, the present results support the existence of a quantum glass transition at x_c . Assuming, based on extrapolation from magnetisation studies for $x < 0.05$ ^{5,6,7,8} and the systematic trends of the μ SR spectra across the many different samples we have so-far investigated, the quantum glass transition is a conventional spin glass transition, in the sense that it has an associated order parameter and symmetry breaking at $T = 0$, then we may interpret the glass transition at $T = 0$ as a quantum critical point.

We note that the values for $T_g(x)$ for $y = 0.05$ are lower than those found in earlier studies for $y = 0.02$ even though $T_g(x)$ was found to increase systematically for $x = 0, 0.01$ and 0.02 ^{25,26}. This presumably occurs because, while Zn slows the spin fluctuations, it also dilutes the spins and at high concentration we see the latter effect. Nevertheless, zinc substitution has undoubtedly exposed the ground state, however distorted it might be, in the samples studied here and allowed us to identify the precise location ($x = 0.19$) at which the spin glass disappears. Based also on the systematic tendency of T_g and T_f to vanish at $x = 0.19$ it is unlikely $y = 0.05$ has suppressed short-range magnetic order only for $x \geq 0.19$. Therefore, we can safely confirm our earlier indications that the magnetic ground state of HTS changes character at x_c , independent of the presence or absence of superconductivity.

Other properties also show distinct changes near x_c . Recent resistivity studies in *both* pure and Zn doped high- T_c oxides showed the transition from a pseudogap towards a Fermi liquid phenomenology⁴¹. Evidence for a change in the ground state has been reported⁴² for the most fundamental measurable quantity in superconductivity, namely the superfluid density

ρ^s . Both the ab -plane and c -axis superfluid response in $\text{La}_{2-x}\text{Sr}_x\text{CuO}_4$ and $\text{HgBa}_2\text{CuO}_{4+\delta}$ were found to remain relatively constant above x_c but drop rapidly below x_c . Furthermore, at 0.19 holes per planar copper atom there is a peak in $\rho^s(0)$ for $\text{HgBa}_2\text{CuO}_{4+\delta}$ indicating the strongest superconductivity at the point where T_g vanishes. Also, the doping dependence of the anisotropy in the penetration depth indicates a crossover from two- to three-dimensional transport. These changes in the superconducting ground state, taken together with the disappearance of the spin glass order at the same doping at $T = 0$, point consistently to a simultaneous change in the ground state symmetry and superconductivity, as expected in a quantum critical point scenario.

In summary, we have suppressed T_c across the superconducting dome of the La-cuprate family. These samples allowed us to take earlier studies a step further and provide new experimental evidence for absence of short-range magnetism for $x \geq 0.19$. The experiments support the presence of a quantum glass transition at $x = 0.19$, as also reflected in the disappearance of spin-glass order and the change in the superconducting ground state.

Acknowledgements: We thank ISIS for the continuing support of this project. C.P. thanks S. Chakravarty and S. Sachdev for useful discussions, and The Royal Society for a University Fellowship. JLT acknowledges financial support from the Marsden Fund.

-
- ¹ S. Sachdev, *Quantum Phase Transitions* (Cambridge University Press 1999).
 - ² V.J. Emery and S.A. Kivelson, J. Phys. Chem. Solids **59**, 1705 (1998).
 - ³ J. Zaanen, J. Phys. Chem. Solids **59**, 1769 (1998).
 - ⁴ C.M. Smith, A.H. Castro Neto and A.V. Balatsky, Phys. Rev. Lett. **87**, 177010 (2001).
 - ⁵ F. C. Chou, N.R. Belk, M.A. Kastner, R.J. Birgeneau and A. Aharony, Phys. Rev. Lett. **75**, 2204 (1995).
 - ⁶ S. Wakimoto, S. Ueki, Y. Endoh and K. Yamada, Phys. Rev. B **62**, 3547 (2000).
 - ⁷ A.N. Lavrov, Y. Ando, S. Komiya and I. Tsukada, Phys. Rev. Lett. **87**, 017007 (2001).
 - ⁸ M.A. Kastner, R.J. Birgeneau, G. Shirane and Y. Endoh, Rev. Mod. Physics **70**, 897 (1998).
 - ⁹ S.F. Edwards and P.W. Anderson, J. Phys. F: Metal Phys. **5**, 965 (1975).
 - ¹⁰ S.F. Edwards and P.W. Anderson, J. Phys. F: Metal Phys. **6**, 1927 (1976).
 - ¹¹ S. Wakimoto, R.J. Birgeneau, Y.S. Lee and G. Shirane, Phys. Rev. B **63**, 172501 (2001).

- ¹² M. Matsuda, M. Fujita, K. Yamada, R.J. Birgeneau, Y. Endoh and G. Shirane, Phys. Rev. B **65**, 134515 (2002).
- ¹³ J. I. Budnick, B. Chamberland, D.P. Yang, C. Niedermayer, A. Golnik, E. Recknagel, M. Rossmanith and A. Wedinger, Europhys. Lett. **5**, 65 (1988).
- ¹⁴ D. R. Harshman *et al.*, Phys. Rev. B **38**, 852 (1988).
- ¹⁵ R.F. Kiefl *et al.*, Phys. Rev. Lett. **63**, 2136 (1989).
- ¹⁶ B.J. Sternlieb *et al.*, Phys. Rev. B **41**, 8866 (1990).
- ¹⁷ Ch. Niedermayer, C. Bernhard, T. Blasius, A. Golnik, A. Moodenbaugh and J.I. Budnick, Phys. Rev. Lett. **80**, 3843 (1998).
- ¹⁸ P. M. Singer and T. Imai, Phys. Rev. Lett. **88**, 187601 (2002).
- ¹⁹ P. M. Singer, A. W. Hunt and T. Imai, Phys. Rev. Lett. **88**, 047602 (2002).
- ²⁰ A. W. Hunt, P. M. Singer, K. R. Thurber and T. Imai, Phys. Rev. Lett. **82**, 4300 (1999).
- ²¹ M.-H. Julien, T. Feher, M. Horvatic, C. Berthier, O.N. Bakharev, P. Segransan, G. Collin and J.F. Marucco, Phys. Rev. Lett. **84**, 3422 (2000).
- ²² M.-H. Julien *et al.*, Phys. Rev. B **63**, 144508 (2001).
- ²³ M.-H. Julien, cond-mat/0211178 at (<http://xxx.lanl.gov>) (2002).
- ²⁴ C. Panagopoulos, B.D. Rainford, J.R. Cooper and C.A. Scott, Physica C **341-348**, 843 (2000).
- ²⁵ C. Panagopoulos, J.L. Tallon, B.D. Rainford, T. Xiang, J.R. Cooper and C.A. Scott, Phys. Rev. B **66**, 064501 (2002).
- ²⁶ C. Panagopoulos, J.L. Tallon, B.D. Rainford, J.R. Cooper, C.A. Scott and T. Xiang, Solid State Comm. **126**, 47 (2003).
- ²⁷ H. Kimura *et al.*, Phys. Rev. B **59**, 6517 (1999).
- ²⁸ B. Nachumi *et al.*, Phys. Rev. B **58**, 8760 (1998).
- ²⁹ Y.J. Uemura, T. Yamazaki, D.R. Harshman, M. Senba and E.J. Ansaldo, Phys. Rev. B **31**, 546 (1985).
- ³⁰ R. Cywinski and B.D. Rainford, Hyperfine Interact. **85**, 215 (1994).
- ³¹ M. Akoshima, Y. Koike, I. Watanabe and K. Nagamine, Phys. Rev. B **62**, 6761 (2000).
- ³² A.T. Savici *et al.*, Phys. Rev. B **66**, 014524 (2002).
- ³³ T. Adachi, I. Watanabe, S.Yairi, K. Takahashi, Y. Koike and K. Nagamine, J. Low Temp. Physics **131**, 843 (2003).
- ³⁴ B. Lake, H.M. Ronnow, N.B. Christensen, G. Aeppli, K. Lefmann, D.F. McMorrow, P. Vorder-

- wisch, P. Smeibidl, N. Mangkorntong, T. Sasagawa, M. Nohara, H. Takagi and T.E. Mason, Nature (London) **415**, 299 (2002).
- ³⁵ S.A. Kivelson, E. Fradkin, V. Oganesyan, I.P. Bindloss, J.M. Tranquada, A. Kapitulnik and C. Howald, Rev. Mod. Physics (in press); cond-mat/0210683 at (<http://xxx.lanl.gov>) (2002).
- ³⁶ A. Kanigel, A. Keren, Y. Eckstein, A. Knizhnik, J.S. Lord and A. Amato, Phys. Rev. Lett. **88**, 137003 (2002).
- ³⁷ A. Keren, A. Kanigel, J.S. Lord and A. Amato, Solid State Comm. **126**, 39 (2003).
- ³⁸ K. Hirota, K. Yamada, I. Tanaka and H. Kojima, Physica B **241**, 817 (1998).
- ³⁹ J. Satooka, Y. Kojima, S. Miyata, K. Suzuki, W. Higemoto, N. Nishiyama and K. Nagamine, Physica B **326**, 585 (2003).
- ⁴⁰ H. Yamagata, H. Miyamoto, K. Nakamura, M. Matsumura and Y. Itoh, J. Phys. Soc. Jpn. **72** (2003) (in press) also cond-mat/0210257 at (<http://xxx.lanl.gov>) (2002).
- ⁴¹ S.H. Naqib, J.R. Cooper, J.L. Tallon and C. Panagopoulos, Physica C, **387**, 365 (2003).
- ⁴² C. Panagopoulos, T. Xiang, W. Anukool, J.R. Cooper, Y.S. Wang and C.W. Chu. Phys. Rev. B **67**, 220502 (2003).

FIGURE CAPTIONS

FIG. 1. The panels on the left-hand-side show zero-field μ SR spectra for $\text{La}_{2-x}\text{Sr}_x\text{Cu}_{0.95}\text{Zn}_{0.05}\text{O}_4$ for $x=0.10 - 0.18$. The solid lines are the fits discussed in the text. The right hand panels show the suppression of the glass transition in presence of longitudinal fields. The solid lines are drawn as guide to the eye. The inset shows oscillations seen for $x=0.10$ and 0.12 at low times. The $x = 0.12$ data have been shifted for clarity. Data were taken at the temperatures indicated in the respective panels.

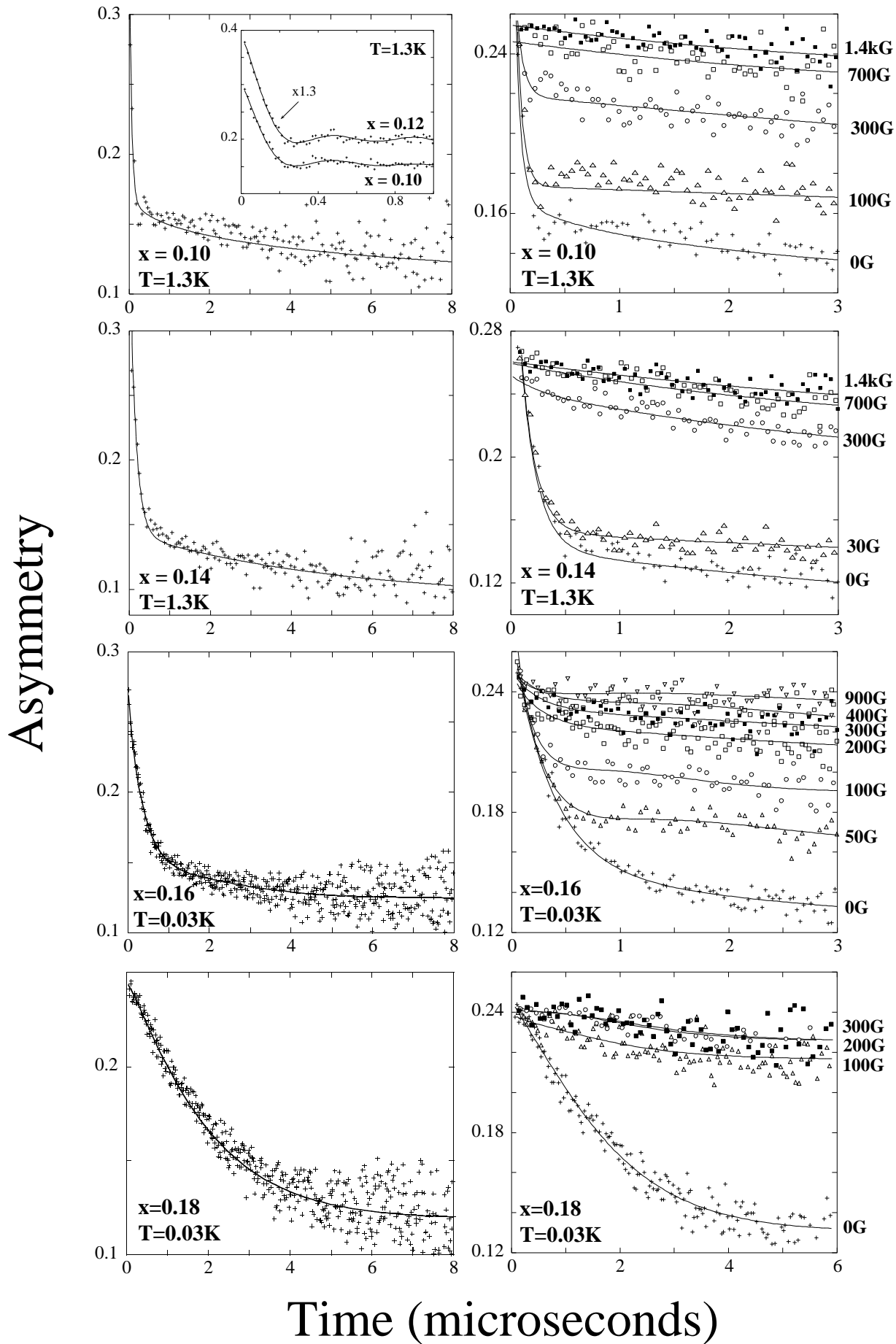
FIG.2. (a) Zero-field μ SR spectra for $\text{La}_{2-x}\text{Sr}_x\text{Cu}_{0.95}\text{Zn}_{0.05}\text{O}_4$ ($x = 0.19$) at different temperatures as indicated in the figure. (b) Suppression of the asymmetry of $x = 0.19$ at $H=30\text{G}$ at two different temperatures (see text for details). (c) Zero-field μ SR spectra for $x=0.10$ measured at different temperatures: $T=1.3\text{K}$ (crosses), 5K (squares), 7K (closed circles), 15K (open circles) and 50K (triangles). (d) Muon asymmetry for $x=0.14$ at high temperature being suppressed by a 30G applied longitudinal field.

FIG. 3. Typical temperature dependence of the (stretched-exponential) exponent β obtained by fitting muon depolarisation data for $\text{La}_{2-x}\text{Sr}_x\text{Cu}_{0.95}\text{Zn}_{0.05}\text{O}_4$ ($x=0.10, 0.14, 0.16, 0.18, 0.19$ and 0.22). The inset to $x=0.10$ shows the temperature dependence of the spin

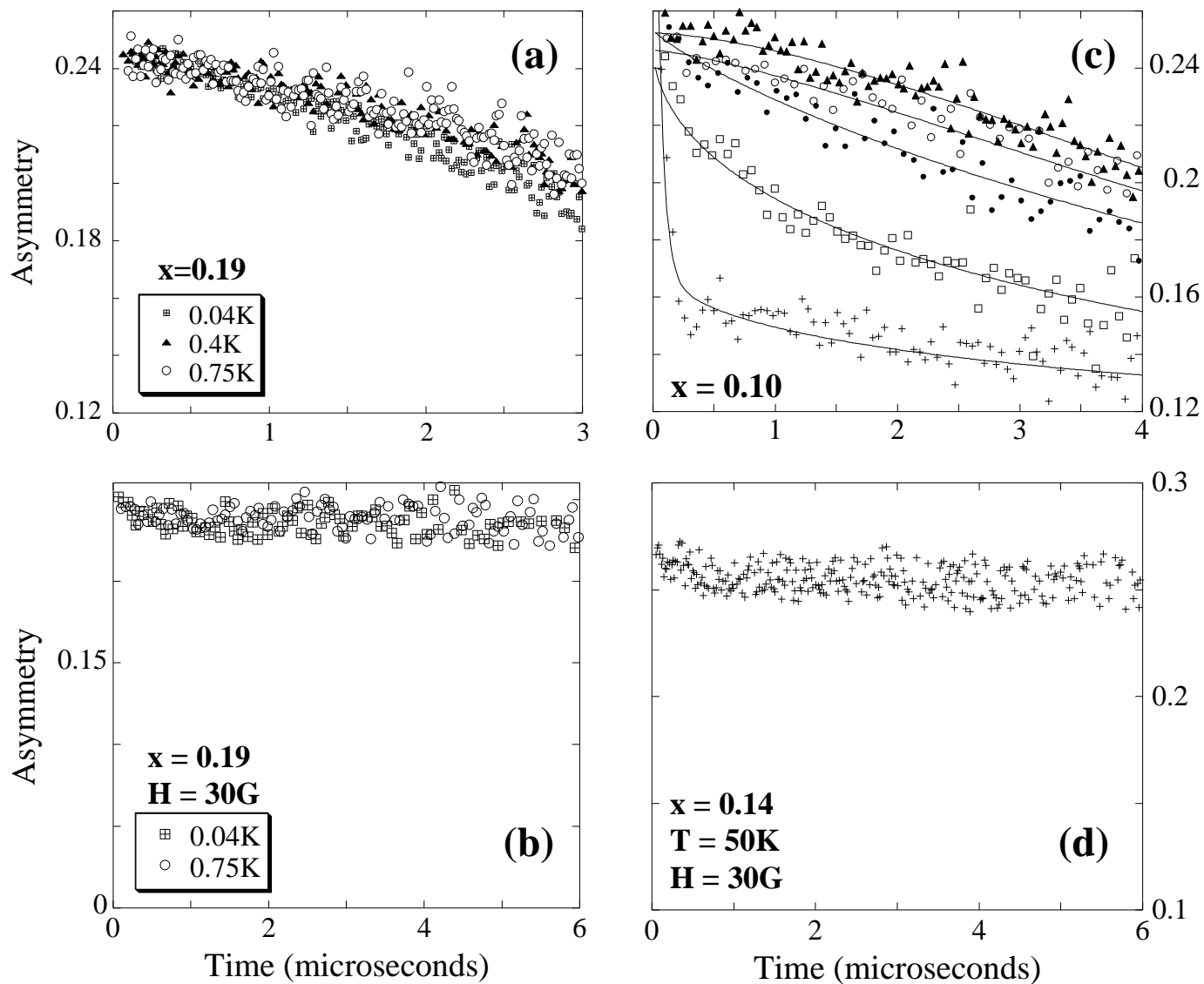
lattice relaxation rate for the same sample.

FIG. 4. The doping dependence of the temperature T_g , below which the spin fluctuations freeze out into a spin glass, for $\text{La}_{2-x}\text{Sr}_x\text{Cu}_{0.95}\text{Zn}_{0.05}\text{O}_4$ ($x=0.10-0.22$). Also shown are data for T_f and B_{local} near x_c .

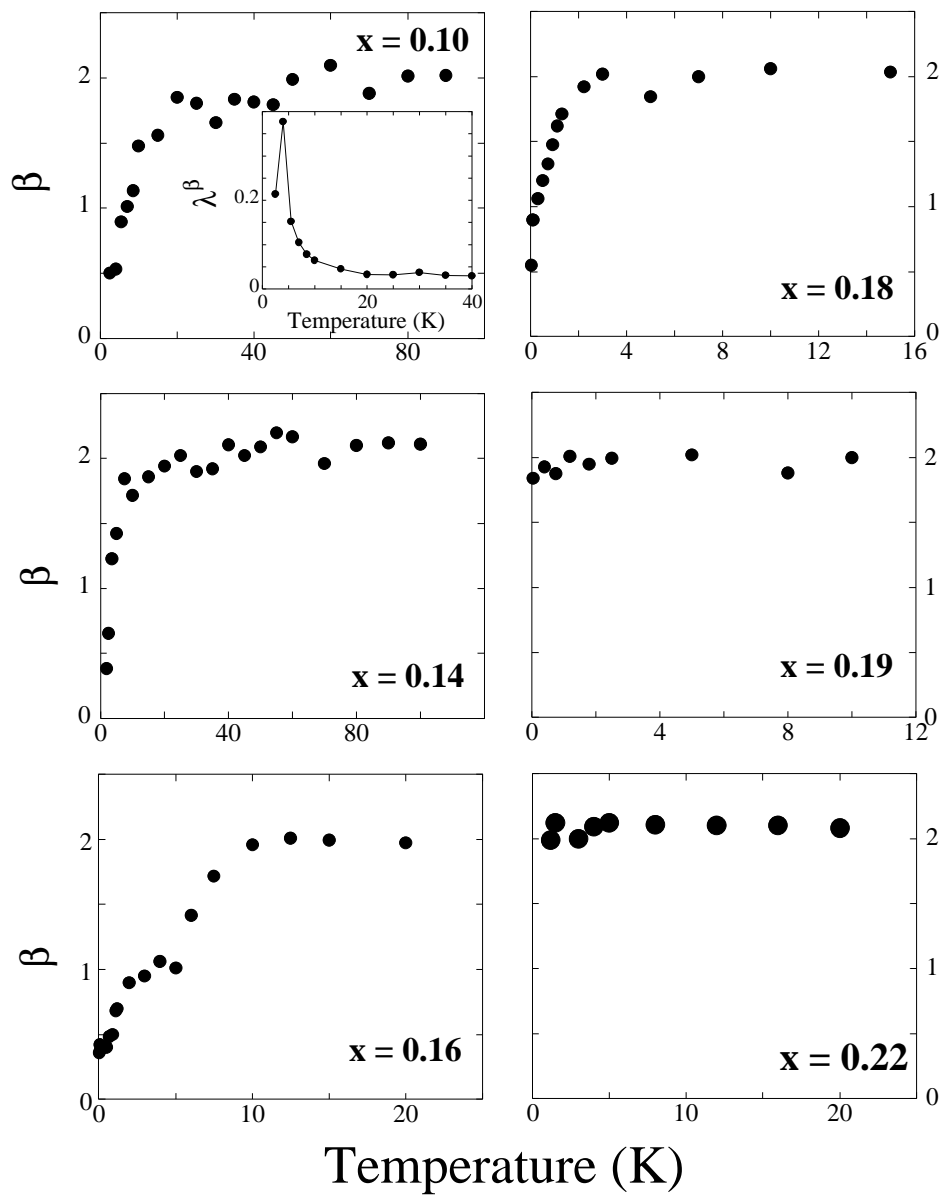
C. Panagopoulos *et al.* Figure 1 revised



C. Panagopoulos *et al.* Figure 2 Revised



C. Panagopoulos *et al.* Figure 3 Revised



C. Panagopoulos *et al.* Figure 4 Revised

